Reconstruction and analysis of a carbon-core metabolic network for Dunaliella salina

Melanie Fachet
Max-Planck-Institut fur Dynamik komplexer technischer Systeme
Carina Witte
Max-Planck-Institut fur Dynamik komplexer technischer Systeme
Robert J Flassig
Technische Hochschule Brandenburg
Liisa K. Rihko-Struckmann (rihko@mpi-magdeburg.mpg.de)
Max-Planck-Institut fur Dynamik komplexer technischer Systeme https://orcid.org/0000-0003-0222-7236
Zaid McKie-Krisberg
Brooklyn College
Juergen EW Polle
Brooklyn College
Kai Sundmacher
Max-Planck-Institut fur Dynamik komplexer technischer Systeme

Research article

Keywords: Dunaliella salina; Metabolic network reconstruction; Central carbon metabolism; Flux balance analysis

Posted Date: October 1st, 2019

DOI: https://doi.org/10.21203/rs.2.9945/v2

Version of Record: A version of this preprint was published on January 2nd, 2020. See the published version at https://doi.org/10.1186/s12859-019-3325-0.

RESEARCH

Reconstruction and validation of a carbon-core metabolic network for Dunaliella salina

Melanie Fachet[1], Carina Witte[1], Robert J Flassig[1,2], Liisa K Rihko-Struckmann[1*], Zaid McKie-Krisberg[3], Jürgen E W Polle[3] and Kai Sundmacher[1,4]

[*]Correspondence:
rihko@mpi-magdeburg.mpg.de
[1]Max Planck Institute for Dynamics of Complex Technical Systems, Process Systems Engineering, Sandtorstr. 1, 39106 Magdeburg, Germany
Full list of author information is available at the end of the article

Abstract

Background: The green microalga *Dunaliella salina* accumulates a high proportion of β-carotene during abiotic stress conditions. To better understand the intracellular flux distribution leading to carotenoid accumulation, this work aimed at reconstructing a carbon core metabolic network for *D. salina* CCAP 19/18 based on the recently published nuclear genome and its validation with experimental observations and literature data.

Results: The reconstruction resulted in a network model with 221 reactions and 212 metabolites within three compartments: cytosol, chloroplast and mitochondrion. The network was implemented in the MATLAB toolbox `CellNetAnalyzer` and checked for feasibility. Furthermore, a flux balance analysis was carried out for different light and nutrient uptake rates. The comparison of the experimental knowledge with the model prediction revealed that the results of the stoichiometric network analysis are plausible and in good agreement with the observed behavior. Accordingly, our model provides an excellent new tool to interrogate and better understand the carbon core metabolism of *D. salina*.

Conclusions: The reconstructed metabolic network of *D. salina* presented in this work is able to predict the biological behavior under light and nutrient stress and will lead to an improved process understanding for the optimized production of high-value products in microalgae.

Keywords: *Dunaliella salina*; Metabolic network reconstruction; Central carbon metabolism; Flux balance analysis

1 Introduction

Microalgae received increased attention over recent years due to their ability to produce high-value compounds such as polyunsaturated fatty acids and carotenoids [1, 2, 3]. Optimizing microalgal growth and product compositions in order to facilitate economically feasible mass production is still challenging. A better understanding of the complex algal metabolism is an important prerequisite to overcome this hurdle. In regards to algal metabolism, the halophilic unicellular green alga *Dunaliella salina* is an excellent model organism to investigate changes in metabolism [4] as the physiology of the switch from primary growth to secondary stress metabolism with glycerol and carotenoid accumulation is very well known [5, 6, 7]. In addition, *D. salina* is still one of the few microalgae being exploited commercialized for β-carotene production on a large scale [8].

The construction of dynamic-kinetic growth models using ordinary differential equations (ODEs) is a well-established formalism in bioprocess engineering. These models allow for prediction of biomass growth, nutrient uptake and metabolite production and enable the identification of bottlenecks in the process setup for lab-scale as well as large-scale outdoor cultivation systems [9, 10, 11]. Although these simplified growth models are robust and computationally inexpensive, they might be only valid for a certain range of environmental conditions and thus have limited predictive capabilities for extrapolation outside the experimental region [12].

It is known that metabolic processes are based on complex reaction pathways throughout different subcellular compartments and its integration into a metabolic model is a prerequisite to get insight into the formation and regulation of metabolites [13]. Several flux-balance models of different plant and algal species have been published. These include models for higher plants *Arabidopsis* [14], barley [15], *Brassica napus* seeds [16] and green microalgae such as *Chlamydomonas* [17, 18, 19, 20, 21], *Chlorella* [22, 23, 24, 25, 26] and *Ostreococcus* [27].

Currently, the productivities of microalgae are still below their actual potential. However, metabolic network reconstructions are the basis for stoichiometric modeling efforts and have the ability to provide theoretical maximal substrate and product yields as well as calculation of internal metabolic rates. Furthermore, they enable in silico identification of genetic intervention strategies that guarantee a specified product yield, e.g. by engineering of the carotenoid or lipid synthesis pathways [28]. Usually, methods such as flux balance analysis (FBA) are used to determine the steady-state flux distribution in a metabolic network under given input conditions by maximization of an objective function. Moreover, extensions for FBA methods such as dynamic flux balance analysis (DFBA) exist accounting for unbalanced growth conditions and dynamic extracellular effects on intracellular metabolism [29, 21]. This enables exploration of metabolic flux distributions consistent with stoichiometric and thermodynamic constraints as well as constraints formulated according to experimental data [30].

Since *D. salina* is the richest source of natural β-carotene, a metabolic network model is highly beneficial to fully exploit the biotechnological potential of this alga. So far, for *D. salina* some metabolic profiling information is available [31, 32], and recently the first growth models had been created [11, 33, 34]. In addition, lately the genome of *D. salina* had been released (http://genome.jgi.doe.gov/DunsalCCAP1918/DunsalCCAP1918 .info.html) [35]. However, the annotation of the nuclear genome is challenging since it contains a high number of long introns and extensive repeats complicating proper gene model construction. Therefore, a genome scale metabolic reconstruction for the industrially relevant microalga *D. salina* is still missing. Based on the nuclear genome of strain CCAP19/18 [35], a manual reconstruction of a carbon-core metabolic network was performed. The aim of the reconstructed stoichiometric network is to describe the metabolic flux distribution leading to the accumulation of the major biomass constituents in *D. salina* under fluctuating light and nutrient conditions.

2 Materials and Methods

2.1 Reconstruction of the stoichiometric network

The stoichiometric model of D. salina CCAP19/18 carbon-core metabolism was reconstructed using a traditional (bottom-up) approach, which was purely based on manual reconstruction. It is based on the assignment of all annotated genes in the nuclear genome of D. salina CCAP19/18 to their proteins and the corresponding reactions supported by biological databases such as KEGG (Kyoto Encyclopedia of Genes and Genomes) [35]. The complete reaction list is given in the Supplementary Material. The graphical representation of the network was created in the vector graphics editor Inkscape (Version 0.92), which is based on[36].

Some metabolites in our stoichiometric network model may have one or more designations denoting its presence in different cellular compartments. Exchange reactions were added allowing the import and export between the considered cellular compartments.

2.2 Implementation and validation of the network

The complete set of reaction equations was implemented in the MATLAB toolbox `CellNetAnalyzer` and checked for feasibility [37]. Unless otherwise stated (e.g. for the nutrient uptake flux or the light flux) the lower and upper bounds for irreversible reactions were fixed to 0 - 100 mmol/(g dw · h) whereas reversible reaction bounds were fixed to -100 - 100 mmol/(g dw · h).

A FBA was carried out for different objective functions as well as light and nutrient uptake rates by using the function `Flux optimization`.

3 Results and discussion

3.1 Reconstruction of a stoichiometric network for the carbon-core metabolism

By linking the annotated genetic information from [35] with bioinformatic knowledge from databases (e.g. KEGG), a stoichiometric network for the carbon-core metabolism with interfaces to amino acid metabolism of *D. salina* CCAP19/18 that comprises 221 reactions and 212 metabolites in three different compartments (chloroplast, cytosol and mitochondrion) was reconstructed. The size of the metabolic network for *D. salina* is in the range of some previously published reduced networks for green microalgae (e.g. for *C. reinhardtii* with 160 reactions, 164 metabolites in 2 compartment by [36] or with 259 reactions, 267 metabolites in 6 compartments by [38]). A comprehensive list of reactions and compounds in the metabolic network can be found in the Supplementary Material. All entries in the list of reactions carrying an EC number (Enzyme commission number) and KEGG ID are annotated enzymes of the *D. salina* genome. Although more extensive metabolic networks exist for a variety of unicellular algae [39, 20, 40], the purpose of our work was to create a first reduced network that would still be capable of predicting biomass composition and productivities.

The central carbon metabolism of green microalgae is generally assumed to be conserved [41, 42]. Fig. 1, 2 and 3 show the network map for the cytosol, the chloroplast and the mitochondrion. To create the metabolic map with subcellular localization of enzymes, the prediction program PredAlgo was used. The prediction tool had been developed and designed to determine the subcellular localization of nuclear-encoded

enzymes in *C. reinhardtii* [43]. For this purpose, PredAlgo distinguishes between the following three compartments: the mitochondrion, the chloroplast, and the cytosol. The study of [43] showed that application of PredAlgo led to an improved discrimination between plastidal and mitochondrial-localized proteins. As stated by the authors, PredAlgo works most accurate for the genus of *Chlamydomonas* and related green algal species (Chlorophyta).

As algae of the genus *Dunaliella* and *Chlamydomonas* are closely related, because they both belong to the order of Volvocales [44], a comparison of annotated enzymes for the calvin cycle, the carbon-core metabolism and the isoprenoid biosynthesis of *D. salina* and *C. reinhardtii* showed a high degree of similarity [41]. In addition, there is a broad consensus that the carbon core metabolisms of green microalgae is conserved along several lineages since almost 90% of the functional annotated proteins of *C. reinhardtii* and of other microalgal proteins are homologs of *Arabidopsis thaliana* proteins [45]. For instance, similar to *C. reinhardtii*, the enzyme triosephosphate isomerase (EC 5.3.1.1) is only present as one gene within the genome of *D. salina*. PredAlgo predicted a chloroplast localization, thus confirming the expected localization with the Calvin-Benson-Bassham cycle for carbon acquisition in the plastid of photosynthetic organisms. Moreover, multiple green algal species (Chlorophyta) share the presence of a glycolytic enolase (EC 4.2.1.11) with cytosolic localization rather than a plastid-localized enolase enzyme [42].

A major difference between the model alga *C. reinhardtii* and *D. salina* is the adaptation of *D. salina* to life under high salinities, whereas *C. reinhardtii* is a soil and/or freshwater alga. Therefore, metabolism of *D. salina* was expected to reveal not only similarities, but also differences in subcellular localization of some of the annotated enzymes. For example, the enzyme the carbonic anhydrase (CA, EC 4.2.1.1) was included in the network to ensure carbon acquisition under high salt conditions. The genome of *C. reinhardtii* contains three α-type, six β-type and three γ-type CAs [46]. In contrast to freshwater species, [47] identified five α-type CAs and three γ-type CAs, but no β-type CAs in *D. salina* CCAP19/18. The newly identified α-type CA (DsCA2b) is suggested to improve CO2 assimilation under hypersaline conditions [47]. Based on results of [48], a plasma membrane localization acting on the extracellular side was assumed. Although a variety of genes code for different classes of carbonic anhydrases [47], we only considered the extracellular version in our model, because it is specific to *Dunaliella*.

In contrast, multiple green algal species (Chlorophyta) share the presence of a glycolytic enolase (EC 4.2.1.11) with cytosolic localization rather than a plastid-localized enolase enzyme [42]. Under hypersaline growth conditions, the osmo-adaptation mechanism in *Dunaliella* leads to a significant glycerol accumulation of up to 30% (w/w) in the biomass depending on the extracellular salt concentration [49]. Although the metabolism of glycerol was thought to be well understood and a glycerol cycle was proposed to exist [50, 51, 52], the aspects of osmosensing and regulation of glycerol metabolism are still only hypotheses [4]. Therefore, our metabolic model placed special emphasis on glycerol metabolism, with glycerol metabolism considered to take place in the cytosol and the chloroplast and linked to the carbon core metabolism of cells as presented in Fig. 1 and 2. Nevertheless, glycerol metabolism is not resolved for the mitochondrion yet.

The glycerol cycle is initiated by the formation of glycerol-3-phosphate from dihydroxyacetone-phosphate, either provided through glycolytic reactions in the cytosol or through the reductive pentose phosphate pathway in the chloroplast [53]. This reversible reaction is catalyzed by the glyceraldehyde-3-phosphate dehydrogenase (GPDH), which exists as two different enzymes, namely Nicotinamide-adenine dinucleotide (NAD+)-dependent enzyme (EC 1.1.1.8) with plastidal and cytosolic localization as well as the ubiquinone-dependent enzyme (EC 1.1.5.3) with cytosolic localization bound to the mitochondrial membrane. The following formation of glycerol from glycerol-3-phosphate was considered to be performed by the glycerol kinase (EC 2.7.1.30). The presented hypothesis of the glycerol cycle within the cytosol also includes the removal of glycerol by conversion to dihydroxyacetone via the dihydroxyacetone reductase (EC 1.1.1.156) and subsequent phosphorylation to dihydroxyacetone-phosphate by the glycerone kinase (EC 2.7.1.29), thus connecting the glycerol cycle back to the glycolysis. Another option for cells to dispose of glycerol may be through general alcohol dehydrogenases (EC 1.1.1.2/1.1.1.21). This is a novel finding, indicating that glycerol could be connected to the carbon core metabolism in more ways than previously proposed, possibly providing a second glycerol cycle in *D. salina*.

Regarding carotenoid biosynthesis, genes coding for all of the enzymes of the plastid localized isoprenoid biosynthesis referred to as the Methyl-Erythritol-Phosphate MEP pathway were identified [35]. In addition, genes for all prenyl transferases needed to synthesize phytoene were found in the genome and all genes coding for enzymes required for reactions leading to β-carotene were identified. This was essential, because under environmental stress cells of *D. salina* de-novo synthezise up to 10% of their dry weight as the isoprenoid molecule β-carotene [5].

Furthermore, the sequencing of various green algal species was an important prerequisite to study the different accumulation patterns of TAGs and carotenoids in green algal species. [54] proposed that the pattern of carbon flow towards TAG or carotenoids is regulated by the NAD(P)H reduction state and the presence of bypass mechanisms such as pyruvate dehydrogenase (PDH). In the case of *D. salina*, the downregulation of PDH induced by high NAD(P)H levels under abiotic stress conditions favors β-carotene hyperaccumulation rather than massive TAG accumulation [54].

3.2 Validation of the stoichiometric network with `CellNetAnalyzer`

The reconstructed network was implemented in the MATLAB toolbox `CellNetAnalyzer` and checked for consistency and feasibility by using the function `Check feasibility of flux scenario`. Additionally, a FBA was carried to out to analyze the plausibility of the flux distribution under varying light and nutrient conditions. The input fluxes for light ($Ex01$) and nutrients ($Ex06$) in the FBA scenarios were fixed according to experimentally obtained values for cultivations in a flat-plate bioreactor setup. For the nitrogen uptake rate, the authors calculated a maximal nitrate uptake rate of 0.19 mmol/(g dw · h) for the nitrogen-replete scenarios and 0.001 mmol/(g dw · h) for the nitrogen-limited scenarios [29]. Additionally, the maximal uptake rate for light ($Ex01$) was adapted to 972 mmol/(g dw · h) according to experimental values obtained in flat-plate bioreactor experiments under high light

conditions [29]. The maintenance ATP requirement (Reaction R191) was calculated by dynamic modeling from chemostat experiments conducted in a laboratory flat-plate bioreactor and was fixed to 0.92 mmol/(g dw · h).

The results of the FBA for the defined scenarios (A-D) are listed in Table 1 and 2. In scenario A, the nitrogen source represented by the metabolite nitrate (NO_3^-) was set to the maximal reaction rate of 0.19 mmol/(g dw · h) to simulate autotrophic growth under nitrogen-replete conditions. For the scenario B, the nitrate flux ($Ex06$) was set to 0.001 mmol/(g dw · h) to simulate autotrophic growth under nitrogen-limited conditions. The objective function was defined to maximize biomass growth (represented by the biomass-forming reaction μ) and the internal fluxes were calculated.

The simulations for the scenarios C and D were carried out under the same nitrogen-replete and depleted conditions as A and B with the only difference that the maximization of the β-carotene flux (`Car14`) was added to the objective function to test whether the flux distribution enables a growth-coupled accumulation of secondary pigments. The objective function for these scenarios is defined as follows: maximization of biomass growth (reaction μ) and β-carotene production (reaction `Car14`).

The resulting growth rates μ for the biomass-maximizing scenarios A and B revealed a nitrogen limited growth regime. Under nitrogen-replete conditions, a growth rate of 0.076 h^{-1} was predicted by the model using a light uptake rate of 696 mmol/(g dw · h) (`Ex01`) which is in the light saturation range for *D. salina* [57]. The predicted growth rate (1.82 d^{-1}) is in line with previously published growth data for *D. salina* CCAP 19/18 where a maximal growth rate of 1.71 d^{-1} was predicted by dynamic-kinetic modeling of batch cultivation data [57]. The calculated growth rate for the nutrient-limited scenario is 0.004 h^{-1} and considerably smaller compared to the nutrient-replete conditions. For maximizing the growth rate under nutrient-limited conditions, the calculated light uptake rate was 972 mmol/(g dw · h) (`Ex01`) which is in the photoinhibition range for *D. salina*. In scenario A and B, biomass production occurred without any formation β-carotene as a side product meaning that the β-carotene flux `Car14` is always 0 mmol/(g dw · h) (Table 1). Since the objective function did only include the biomass growth (μ) under nitrogen-replete conditions it is biologically plausible that β-carotene formation was suppressed in flux scenario A. As described by [6] and [11] oversaturating light conditions and nutrient repletion led only to moderate β-carotene accumulation whereas light stress combined with nutrient stress is the most potent inducer of secondary carotenoids in *D. salina*.

In the tested scenarios C and D (Table 2), which were similar to A and B unless the extension of the objective function to maximize the β-carotene flux (`Car14`), the same growth rates as in scenario A and B were calculated (0.076 h^{-1} for nutrient-replete conditions and 0.004 h^{-1} for nutrient-limited conditions). However, the predicted β-carotene flux was different compared to scenario A and B. Whereas for the nutrient-replete scenario a β-carotene flux (`Car14`) of 1.46 mmol/(g dw · h) was predicted, it increased to 1.94 mmol/(g DW h) under nutrient-limited conditions (Table 2). The calculated light flux for both scenarios was 844 mmol/(g dw · h) which corresponds to a high light cultivation condition. This is in line with the biological function of β-carotene as a light stress-induced secondary pigment to minimize

the damaging effects of oversaturating light on the cellular metabolism even under nitrogen-replete conditions. The absence of biomass production in scenario B and D is plausible, since nitrogen depletion leads to inhibition of protein biosynthesis which is a prerequiste for growth. Moreover, it is known that β-carotene accumulation is induced by nutrient stress and can act as a metabolic sink to avoid end-product inhibition [56].

4 Conclusion

This work presents a metabolic network reconstruction of the carbon-core metabolism of *D. salina* CCAP19/18 based on the recently announced annotated genome [35]. The network comprises 221 reactions with 212 metabolites in three compartments (chloroplast, cytsol and mitochondrion). The network was implemented in the MATLAB toolbox `CellNetAnalyzer` and a flux balance analysis was carried out under various light and nutrient scenarios. The simulation results were compared with experimental observations of *D. salina* cultivated under nutrient repletion and depletion in a flat-plate photobioreactor [57]. All model predictions could be confirmed by experimental data and biological knowledge of *D. salina* metabolism. In conclusion, the metabolic network reconstruction is suitable to gain a better understanding of the flux distribution in the carbon core metabolism during carotenogenesis in *D. salina*. The ongoing experimental and computational advances will thereby accelerate the engineering of industrially valuable strains and provides the basis for effective biotechnology with photosynthetic microorganisms.

Competing interests
The authors declare that they have no competing interests.

Author's contributions
ZMKK and JEWP provided the annotated genetic information for *D. salina* CCAP19/18. MF and CW reconstructed the stoichiometric network model, implemented it in `CellNetAnalyzer` and carried out the FBA. RJF, LRS and KS designed the research concept and revised the manuscript. All authors read and approved the final manuscript.

Acknowledgements
We would like to thank Steffen Klamt for pointing out some inconsistencies in the FBA model.

Funding
This research work was partly supported by the Center for Dynamic Systems (CDS) funded by the Federal State Saxony-Anhalt (Germany).

Availability of data and materials
The datasets used and/or analyzed during the current study are available from the corresponding author on reasonable request.

Consent for publication
Not applicable.

Ethics approval and consent to participate
Not applicable.

Author details
[1]Max Planck Institute for Dynamics of Complex Technical Systems, Process Systems Engineering, Sandtorstr. 1, 39106 Magdeburg, Germany. [2]Brandenburg University of Applied Sciences, Department of Engineering, Magdeburger Str. 50, 14770 Brandenburg an der Havel, Germany. [3]Brooklyn College of the City University of New York, Department of Biology, 2900 Bedford Avenue, NY 11210 New York, USA. [4]Otto von Guericke University Magdeburg, Process Systems Engineering, Universitätsplatz 2, 39106 Magdeburg, Germany.

References

1. Borowitzka, M.A.: Commercial production of microalgae: ponds, tanks, tubes and fermenters. Journal of Biotechnology **70**(1), 313–321 (1999). doi:10.1016/S0168-1656(99)00083-8. Biotechnological Aspects of Marine Sponges

2. Adarme-Vega, T.C., Lim, D.K.Y., Timmins, M., Vernen, F., Li, Y., Schenk, P.M.: Microalgal biofactories: a promising approach towards sustainable omega-3 fatty acid production. Microbial Cell Factories **11**(1), 96 (2012). doi:10.1186/1475-2859-11-96
3. Khan, M.I., Shin, J.H., Kim, J.D.: The promising future of microalgae: current status, challenges, and optimization of a sustainable and renewable industry for biofuels, feed, and other products. Microbial Cell Factories **17**(1), 36 (2018). doi:10.1186/s12934-018-0879-x
4. Ramos, A.: The unicellular green alga *Dunaliella salina* Teod. as a model for abiotic stress tolerance: Genetic advances and future perspectives. Algae **26**(1), 3–20 (2011). doi:10.4490/algae.2011.26.1.003
5. Ben-Amotz, A., Avron, M.: On the factors which determine massive β-carotene accumulation in the halotolerant alga *Dunaliella bardawil*. Plant Physiol **72**(3), 593–7 (1983)
6. Lamers, P.P., van de Laak, C.C.W., Kaasenbrood, P.S., Lorier, J., Janssen, M., De Vos, R.C.H., Bino, R.J., Wijffels, R.H.: Carotenoid and fatty acid metabolism in light-stressed *Dunaliella salina*. Biotechnology and Bioengineering **106**(4), 638–648 (2010)
7. Lamers, P.P., Janssen, M., De Vos, R.C.H., Bino, R.J., Wijffels, R.H.: Carotenoid and fatty acid metabolism in nitrogen-starved *Dunaliella salina*, a unicellular green microalga. Journal of Biotechnology **162**(1), 21–27 (2012). doi:10.1016/j.jbiotec.2012.04.018
8. Borowitzka, M.A.: High-value products from microalgae - their development and commercialisation. Journal of Applied Phycology **25**(3), 743–756 (2013). doi:10.1007/s10811-013-9983-9
9. Packer, A., Li, Y., Andersen, T., Hu, Q., Kuang, Y., Sommerfeld, M.: Growth and neutral lipid synthesis in green microalgae: A mathematical model. Bioresource Technology **102**(1), 111–7 (2011)
10. Quinn, J., de Winter, L., Bradley, T.: Microalgae bulk growth model with application to industrial scale systems. Bioresource Technology **102**(8), 5083–92 (2011). doi:10.1016/j.biortech.2011.01.019
11. Fachet, M., Flassig, R.J., Rihko-Struckmann, L., Sundmacher, K.: A dynamic growth model of *Dunaliella salina*: Parameter identification and profile likelihood analysis. Bioresource Technology **173C**, 21–31 (2014). doi:10.1016/j.biortech.2014.08.124
12. Mairet, F., Bernard, O., Masci, P., Lacour, T., Sciandra, A.: Modelling neutral lipid production by the microalga *Isochrysis* aff. *galbana* under nitrogen limitation. Bioresource Technology **102**(1), 142–149 (2011)
13. Yu, W.-L., Ansari, W., Schoepp, N.G., Hannon, M.J., Mayfield, S.P., Burkart, M.D.: Modifications of the metabolic pathways of lipid and triacylglycerol production in microalgae. Microbial Cell Factories **10**(1), 91 (2011). doi:10.1186/1475-2859-10-91
14. de Oliveira Dal'Molin, C.G., Quek, L.-E., Palfreyman, R.W., Brumbley, S.M., Nielsen, L.K.: AraGEM, a genome-scale reconstruction of the primary metabolic network in *Arabidopsis*. Plant Physiology **152**(2), 579–589 (2010). doi:10.1104/pp.109.148817. http://www.plantphysiol.org/content/152/2/579.full.pdf
15. Grafahrend-Belau, E., Junker, A., Eschenröder, A., Müller, J., Schreiber, F., Junker, B.H.: Multiscale metabolic modeling: Dynamic flux balance analysis on a whole-plant scale. Plant Physiology **163**(2), 637–647 (2013). doi:10.1104/pp.113.224006
16. Jordan, H., Jörg, S.: Computational analysis of storage synthesis in developing *Brassica napusj* l. (oilseed rape) embryos: Flux variability analysis in relation to 13C metabolic flux analysis. The Plant Journal **67**(3), 513–525 (2011). doi:10.1111/j.1365-313X.2011.04611.x
17. Boyle, N.R., Morgan, J.A.: Flux balance analysis of primary metabolism in *Chlamydomonas reinhardtii*. BMC Systems Biology **3**, 4 (2009). doi:10.1186/1752-0509-3-4
18. Chang, R.L., Ghamsari, L., Manichaikul, A., Hom, E.F., Balaji, S., Fu, W., Shen, Y., Hao, T., Palsson, B.O., Salehi-Ashtiani, K., Papin, J.A.: Metabolic network reconstruction of *Chlamydomonas* offers insight into light-driven algal metabolism. Molecular Systems Biology **7**, 518 (2011)
19. Dal'Molin, C.G., Quek, L.E., Palfreyman, R.W., Nielsen, L.K.: AlgaGEM - a genome-scale metabolic reconstruction of algae based on the *Chlamydomonas reinhardtii* genome. BMC Genomics **12**(4), 1–10 (2011)
20. Saheed, I., Sascha, S., Jacob, V., de Lomana Adrian, L.G., Warren, C., D., P.N., S., B.N.: A refined genome-scale reconstruction of *Chlamydomonas* metabolism provides a platform for systems-level analyses. The Plant Journal **84**(6), 1239–1256 (2015). doi:10.1111/tpj.13059
21. Mora Salguero, D.A., Fernández-Niño, M., Serrano-Bermúdez, L.M., Páez Melo, D.O., Winck, F.V., Caldana, C., González Barrios, A.F.: Development of a *Chlamydomonas reinhardtii* metabolic network dynamic model to describe distinct phenotypes occurring at different CO2,) levels. PeerJ **6**(e5528), 1–25 (2018). doi:10.7717/peerj.5528
22. Yang, C., Hua, Q., Shimizu, K.: Energetics and carbon metabolism during growth of microalgal cells under photoautotrophic, mixotrophic and cyclic light-autotrophic/dark-heterotrophic conditions. Biochemical Engineering Journal **6**(2), 87–102 (2000)
23. Muthuraj, M., Palabhanvi, B., Misra, S., Kumar, V., Sivalingavasu, K., Das, D.: Flux balance analysis of *Chlorella* sp. FC2 IITG under photoautotrophic and heterotrophic growth conditions. Photosynthesis Research **118**(1-2), 167–79 (2013). doi:10.1007/s11120-013-9943-x
24. Wu, C., Xiong, W., Dai, J., Wu, Q.: Genome-based metabolic mapping and 13C flux analysis reveal systematic properties of an oleaginous microalga *Chlorella protothecoides*. Plant Physiology **167**(2), 586–99 (2015). doi:10.1104/pp.114.250688
25. Zhu, Y., Huang, Y.: Use of flux balance analysis to promote lipid productivity in *Chlorella sorokiniana*. Journal of Applied Phycology **29**(2), 889–902 (2017). doi:10.1007/s10811-016-0973-6
26. Parichehreh, R., Gheshlaghi, R., Mahdavi, M.A., Elkamel, A.: Optimization of lipid production in chlorella vulgaris for biodiesel production using flux balance analysis. Biochemical Engineering Journal **141**, 131–145 (2019). doi:10.1016/j.bej.2018.10.011
27. Krumholz, E.W., Yang, H., Weisenhorn, P., Henry, C.S., Libourel, I.G.L.: Genome-wide metabolic network reconstruction of the picoalga *Ostreococcus*. Journal of Experimental Botany **63**(6), 2353–2362 (2012)
28. Gimpel, J.A., Henriquez, V., Mayfield, S.P.: In metabolic engineering of eukaryotic microalgae: Potential and challenges come with great diversity. Frontiers in Microbiology **6**, 1376 (2015)
29. Flassig, R.J., Fachet, M., Höffner, K., Barton, P.I., Sundmacher, K.: Dynamic flux balance modeling to increase

the production of high-value compounds in green microalgae. Biotechnology for Biofuels **9**(1), 1–12 (2016). doi:10.1186/s13068-016-0556-4
30. Höffner, K., Harwood, S.M., Barton, P.I.: A reliable simulator for dynamic flux balance analysis. Biotechnology and Bioengineering **110**(3), 792–802 (2013). doi:10.1002/bit.24748
31. Samburova, V., Lemos, M.S., Hiibel, S., Kent Hoekman, S., Cushman, J.C., Zielinska, B.: Analysis of triacylglycerols and free fatty acids in algae using ultra-performance liquid chromatography mass spectrometry. Journal of the American Oil Chemists' Society **90**(1), 53–64 (2013). doi:10.1007/s11746-012-2138-3
32. Lv H, W.S. Cui X, S, J.: Metabolic profiling of *Dunaliella salina* shifting cultivation conditions to nitrogen deprivation. Metabolomics:Open Access **6**(1), (2016). doi:10.4172/2153-0769.1000170
33. Bechet, Q., Moussion, P., Bernard, O.: Calibration of a productivity model for the microalgae *Dunaliella salina* accounting for light and temperature. Algal Research **21**, 156–160 (2017). doi:10.1016/j.algal.2016.11.001
34. Bechet, Q., Coulombier, N., Vasseura, C., Lasserre, T., Le Dean, L., Bernard, O.: Full-scale validation of an algal productivity model including nitrogen limitation. Algal Research **31**, 377–386 (2018). doi:10.1016/j.algal.2018.02.010
35. Polle, J.E.W., Barry, K., Cushman, J., Schmutz, J., Tran, D., Hathwaik, L.T., Yim, W.C., Jenkins, J., McKie-Krisberg, Z., Prochnik, S., Lindquist, E., Dockter, R.B., Adam, C., Molina, H., Bunkenborg, J., Jin, E., Buchheim, M., Magnuson, J.: Draft Nuclear Genome Sequence of the Halophilic and Beta-Carotene-Accumulating Green Alga *Dunaliella salina* Strain CCAP19/18. Genome Announc **5**(43) (2017)
36. Kliphuis, A., Klok, A., Martens, D., Lamers, P., Janssen, M., Wijffels, R.: Metabolic modeling of *Chlamydomonas reinhardtii*: Energy requirements for photoautotrophic growth and maintenance. Journal of Applied Phycology **24**(2), 253–266 (2011). doi:10.1007/s10811-011-9674-3
37. Klamt, S., Saez-Rodriguez, J., Gilles, E.D.: Structural and functional analysis of cellular networks with CellNetAnalyzer. BMC Systems Biology **1**, 2 (2007)
38. Manichaikul, A., Ghamsari, L., Hom, E.F., Lin, C., Murray, R.R., Chang, R.L., Balaji, S., Hao, T., Shen, Y., Chavali, A.K., Thiele, I., Yang, X., Fan, C., Mello, E., Hill, D.E., Vidal, M., Salehi-Ashtiani, K., Papin, J.A.: Metabolic network analysis integrated with transcript verification for sequenced genomes. Nature Methods **6**(8), 589–92 (2009). doi:10.1038/nmeth.1348
39. Reijnders, M.J.M.F., van Heck, R.G.A., Lam, C.M.C., Scaife, M.A., Santos, V.A.P.M.d., Smith, A.G., Schaap, P.J.: Green genes: Bioinformatics and systems-biology innovations drive algal biotechnology. Trends in Biotechnology **32**(12), 617–626 (2014). doi:10.1016/j.tibtech.2014.10.003
40. Loira, N., Mendoza, S., Paz Cortas, M., Rojas, N., Travisany, D., Genova, A.D., Gajardo, N., Ehrenfeld, N., Maass, A.: Reconstruction of the microalga *Nannochloropsis salina* genome-scale metabolic model with applications to lipid production. BMC Systems Biology **11**(1), 66 (2017)
41. Xenie, J., Jean, A.: Central carbon metabolism and electron transport in *Chlamydomonas reinhardtii*: Metabolic constraints for carbon partitioning between oil and starch. Eukaryotic Cell **12**(6), 776–93 (2013). doi:10.1128/EC.00318-12
42. Polle, J.E.W., Neofotis, P., Huang, A., Chang, W., Sury, K., Wiech, E.M.: Carbon partitioning in green algae (Chlorophyta) and the enolase enzyme. Metabolites **4**(3), 612–28 (2017). doi:10.3390/metabo4030612
43. Tardif, M., Atteia, A., Specht, M., Cogne, G., Rolland, N., Brugiere, S., Hippler, M., Ferro, M., Bruley, C., Peltier, G., Vallon, O., Cournac, L.: PredAlgo: A new subcellular localization prediction tool dedicated to green algae. Molecular biology and evolution **29**(12), 3625–39 (2012). doi:10.1093/molbev/mss178
44. Gonzalalez, M.A., Gomez, P.I., E. W. Polle, J.: In: Ben-Amotz, A..E.W.P.J..S.R.D.V. (ed.) Taxonomy and Phylogeny of the Genus *Dunaliella*, 1st edn. Science Publishers, Enfield (2009). Chap. 15-43
45. Reijnders, M.J.M.F., Carreres, B.M., Schaap, P.J.: Algal Omics: The functional annotation challenge. Current Biotechnology **4**(4), 457–463 (2015)
46. Moroney, J., Yunbing, M., Frey, W.D., Fusilier, K.A., Pham, T.T., Simms, T., Dimario, R.J., Yang, J., Mukherjee, B.: The carbonic anhydrase isoforms of *Chlamydomonas reinhardtii*: Intracellular location, expression, and physiological roles. Photosynthesis research **109**, 133–49 (2011). doi:10.1007/s11120-011-9635-3
47. Jeon, H., Jeong, J., Baek, K., McKie-Krisberg, Z., Polle, J.E.W., Jin, E.: Identification of the carbonic anhydrases from the unicellular green alga *Dunaliella salina* strain CCAP 19/18. Algal Research **19**, 12–20 (2016). doi:10.1016/j.algal.2016.07.010
48. Premkumar, L., Bageshwar, U.K., Gokhman, I., Zamir, A., J.L., S.: An unusual halotolerant α-type carbonic anhydrase from the alga *Dunaliella salina* functionally expressed in *Escherichia coli*. Protein Expression and Purification **28**(1), 151–157 (2003). doi:10.1016/S1046-5928(02)00683-6
49. Ben-Amotz, A., Avron, M.: The role of glycerol in the osmotic regulation of the halophilic alga *Dunaliella parva*. Plant Physiology **51**(5), 875–878 (1973). doi:10.1104/pp.51.5.875. http://www.plantphysiol.org/content/51/5/875.full.pdf
50. Ben-Amotz A., A.M. Sussman I.: Glycerol production by *Dunaliella*. Experientia **38**(1), 49–52 (1982)
51. Chen, H., Lu, Y., Jiang, J.G.: Comparative analysis on the key enzymes of the glycerol cycle metabolic pathway in *Dunaliella salina* under osmotic stresses. PLoS ONE **7**(6), 37578 (2012)
52. K., W.: Osmotic regulation of photosynthetic glycerol production in *Dunaliella*. Bioenergetics **234**(3), 317–323 (1971)
53. Chitlaru, E., Pick, U.: Regulation of glycerol synthesis in response to osmotic changes in *Dunaliella*. Plant Physiology **96**(1), 50–60 (1991). doi:10.1104/pp.96.1.50. http://www.plantphysiol.org/content/96/1/50.full.pdf
54. McKie-Krisberg, Z., Laurens, L., Huang, A., Polle, J.E.W.: Comparative energetics of carbon storage molecules in green algae. Algal Research **31**, 326–333 (2018). doi:10.1016/j.algal.2018.01.018
55. Cifuentes, A.S., Gonzalez, M., Conejeros, M., Dellarossa, V., Parra, O.: Growth and carotenogenesis in eight strains of *Dunaliella salina* Teodoresco from Chile. Journal of Applied Phycology **4**(2), 111 (1992). doi:10.1007/bf02442459
56. Rabbani, S., Beyer, P., Von Lintig, J., Hugueney, P., Kleinig, H.: Induced β-carotene synthesis driven by

triacylglycerol deposition in the unicellular alga *Dunaliella bardawil*. Plant Physiology **116**(4), 1239–1248 (1998)

57. Fachet, M., Flassig, R.J., Rihko-Struckmann, L.K., Sundmacher, K.: Carotenoid production process using green microalgae of the *Dunaliella* genus: Model-based analysis of interspecies variability. Industrial & Engineering Chemistry Research **56**(45), 12888–12898 (2017). doi:10.1021/acs.iecr.7b01423

Figures

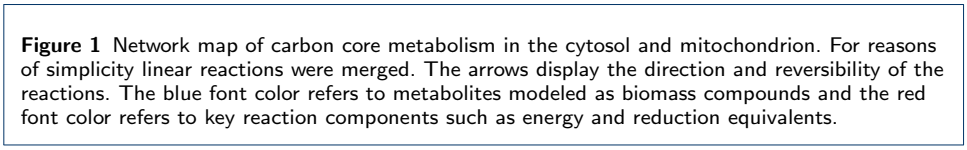

Figure 1 Network map of carbon core metabolism in the cytosol and mitochondrion. For reasons of simplicity linear reactions were merged. The arrows display the direction and reversibility of the reactions. The blue font color refers to metabolites modeled as biomass compounds and the red font color refers to key reaction components such as energy and reduction equivalents.

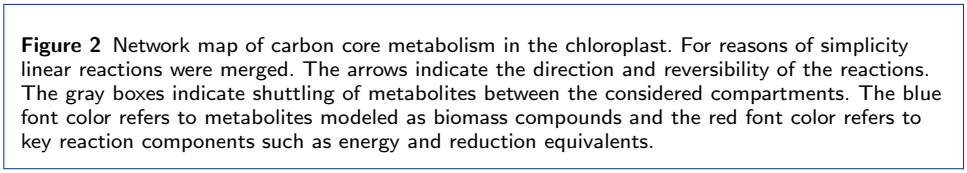

Figure 2 Network map of carbon core metabolism in the chloroplast. For reasons of simplicity linear reactions were merged. The arrows indicate the direction and reversibility of the reactions. The gray boxes indicate shuttling of metabolites between the considered compartments. The blue font color refers to metabolites modeled as biomass compounds and the red font color refers to key reaction components such as energy and reduction equivalents.

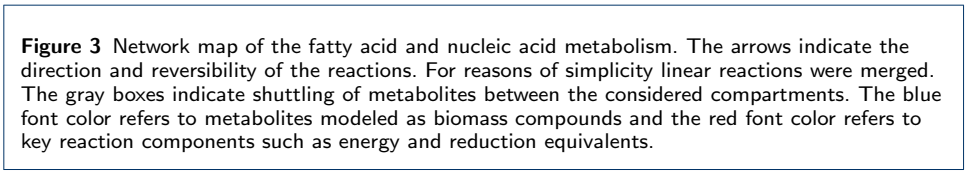

Figure 3 Network map of the fatty acid and nucleic acid metabolism. The arrows indicate the direction and reversibility of the reactions. For reasons of simplicity linear reactions were merged. The gray boxes indicate shuttling of metabolites between the considered compartments. The blue font color refers to metabolites modeled as biomass compounds and the red font color refers to key reaction components such as energy and reduction equivalents.

Tables

Table 1 Input conditions and predicted growth rates for the defined scenario A and B

Scenario	A	B
Condition	nitrogen-replete	nitrogen-depleted
Input conditions:		
Nutrients (NO_3^-)	0.19	0.001
Objective function		max(μ)
Calc. growth rate in 1/h	0.076	0.0004
Calc. light uptake rate (`Ex01`)	696	972
Calc. β-carotene production in mmol/(g dw · h)	0	0

Table 2 Input conditions and predicted growth rates for the defined scenario C and D

Scenario	C	D
Condition	nitrogen-replete	nitrogen-depleted
Input conditions:		
Nutrients (NO_3^-)	0.19	0.001
Objective function		max(μ,`Car14`)
Calc. growth rate in 1/h	0.076	0.0004
Calc. light uptake rate (`Ex01`)	844	844
Calc. β-carotene production in mmol/(g dw · h)	1.46	1.94

Additional Files

Additional file 1 - List of reactions, metabolites and biomass composition
Additional file 2 - SBML Model
Additional file 3 - Graphical representation of flux scenarios

Figures

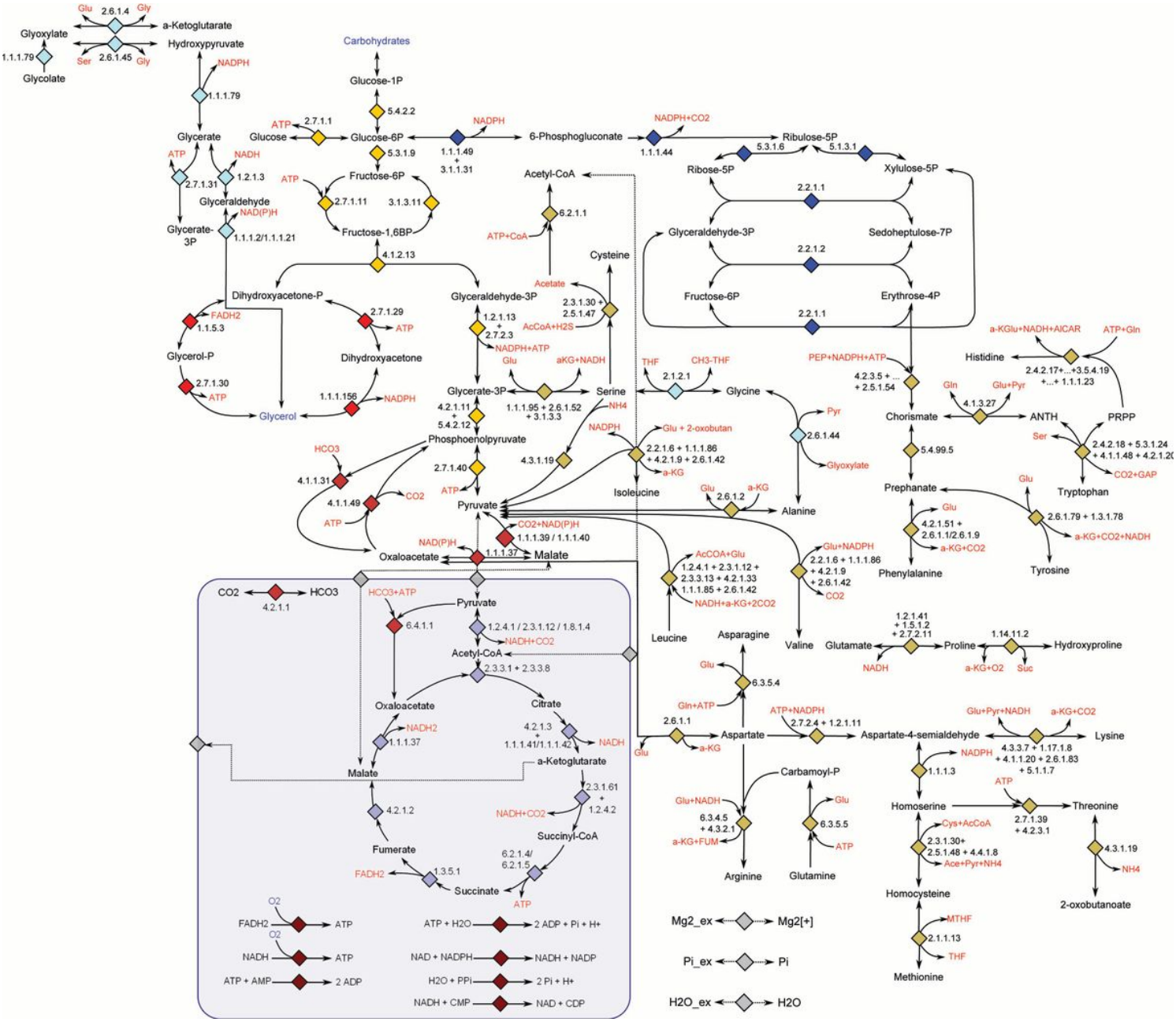

Figure 1

Network map of carbon core metabolism in the cytosol and mitochondrion. For reasons of simplicity linear reactions were merged. The arrows display the direction and reversibility of the reactions. The blue font color refers to metabolites modeled as biomass compounds and the red font color refers to key reaction components such as energy and reduction equivalents.

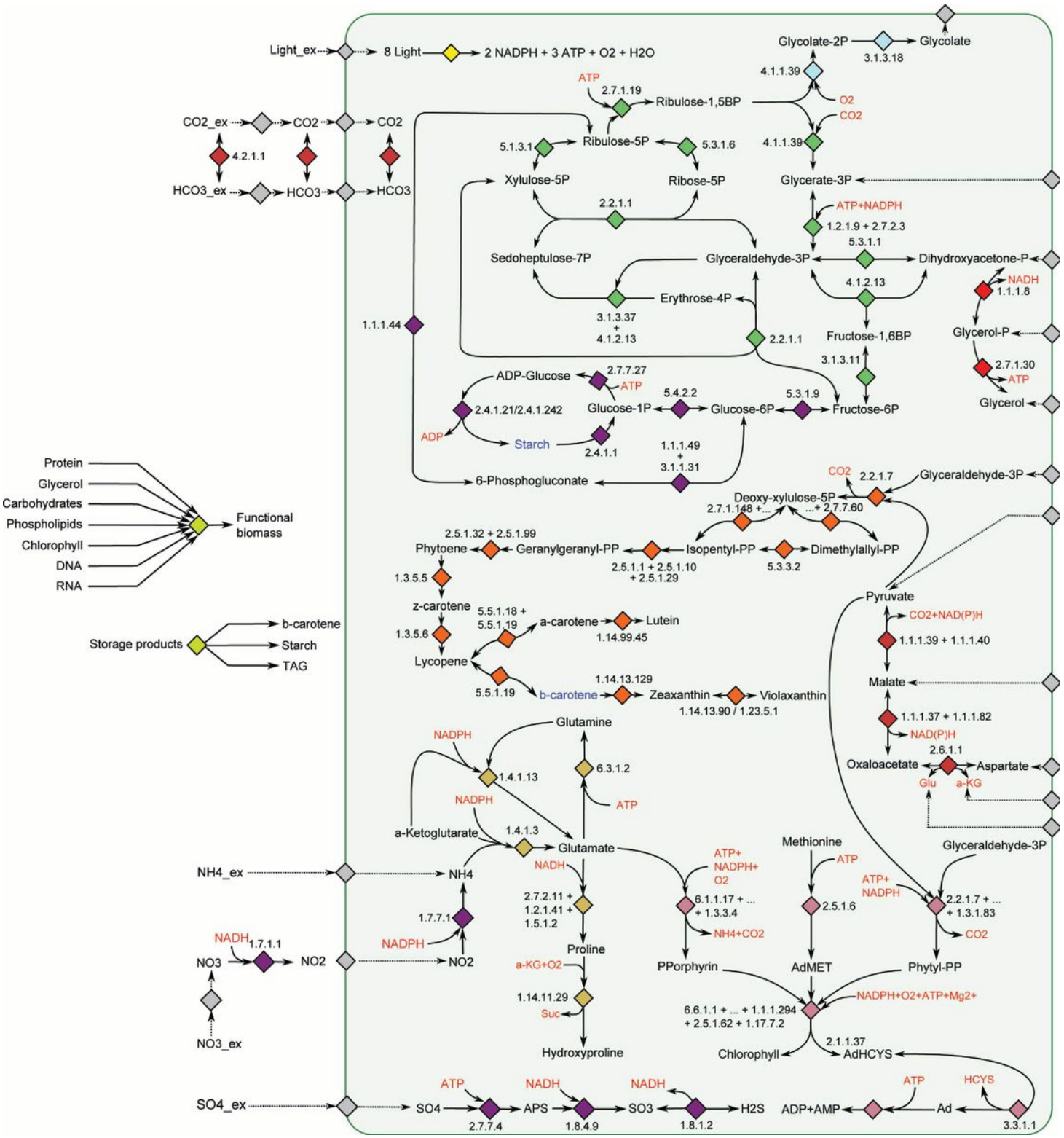

Figure 2

Network map of carbon core metabolism in the chloroplast. For reasons of simplicity linear reactions were merged. The arrows indicate the direction and reversibility of the reactions. The gray boxes indicate shuttling of metabolites between the considered compartments. The blue font color refers to metabolites modeled as biomass compounds and the red font color refers to key reaction components such as energy and reduction equivalents.

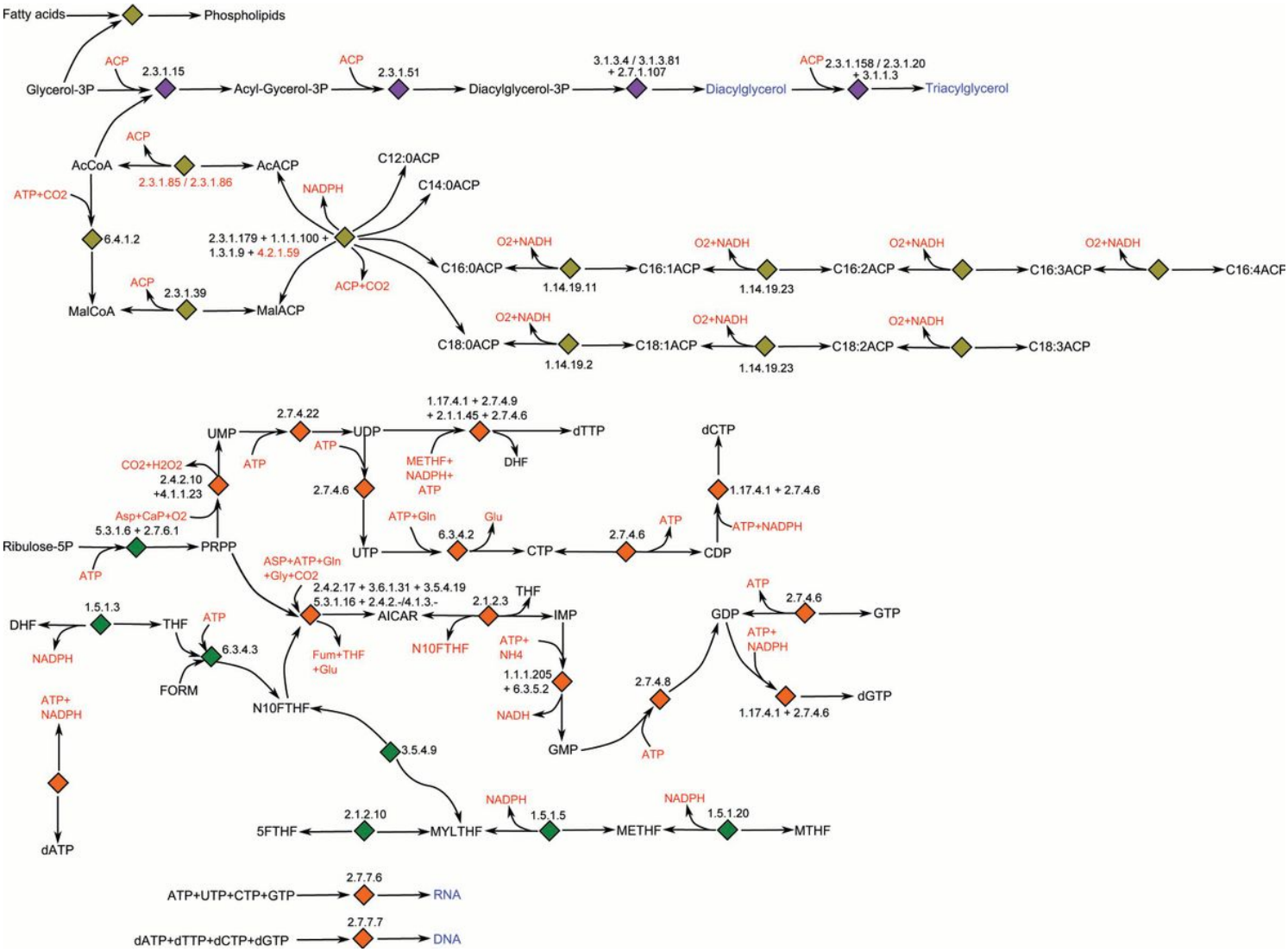

Figure 3

Network map of the fatty acid and nucleic acid metabolism. The arrows indicate the direction and reversibility of the reactions. For reasons of simplicity linear reactions were merged. The gray boxes indicate shuttling of metabolites between the considered compartments. The blue font color refers to metabolites modeled as biomass compounds and the red font color refers to key reaction components such as energy and reduction equivalents.

Supplementary Files

This is a list of supplementary files associated with this preprint. Click to download.

- Dsalina190517.xml
- Fluxscenarios.zip
- Supp1ReactionsBiomass.pdf